



## Development and characterization of shape memory Cu–Zn–Al thin films

N. Haberkorn<sup>a,b,\*</sup>, F.C. Lovey<sup>a,b</sup>, A.M. Condó<sup>a,b</sup>, J. Guimpel<sup>a,b</sup>

<sup>a</sup> Comisión Nacional de Energía Atómica, Centro Atómico Bariloche, S. C. de Bariloche, 8400 R. N., Argentina

<sup>b</sup> Instituto Balseiro, Universidad Nacional de Cuyo and Comisión Nacional de Energía Atómica, S. C. de Bariloche, 8400 R. N., Argentina

### ARTICLE INFO

#### Article history:

Received 15 September 2009

Received in revised form 21 January 2010

Accepted 27 January 2010

#### Keywords:

Thin films

Shape memory

Cu–Zn–Al

### ABSTRACT

Ternary Cu–Zn–Al alloys show good shape memory properties with narrow hysteresis and a wide range of martensitic transformation temperature ( $M_s$ ), depending on the alloy composition. Thin films of Cu–Zn–Al with shape memory effect were grown for the first time using a new procedure. First Cu–Al thin films were obtained by DC sputtering on Si (100) substrates at room temperature, and second, the Cu–Al films were encapsulated and annealed in the presence of a Cu–Zn–Al bulk reference in order to fix a Zn vapour pressure. In this way a controlled amount of Zn is transported from the bulk reference into the film, in such a way that the  $M_s$  of the film becomes nearly the same as the bulk reference. The structures and microstructures of the as grown films were analysed by X-ray diffraction and transmission electron microscopy. The martensitic transformation temperature was determined by resistivity measurements.

© 2010 Elsevier B.V. All rights reserved.

### 1. Introduction

Many materials undergo a first-order diffusionless phase transformation consisting in a sudden change of the crystal structure at a certain temperature, which is called martensitic transformation. As a consequence a macroscopic shape change of the material can be observed. In the last years, thin films of shape memory alloys (SMA) have been recognized as promising and high performance materials in the field of microelectromechanical systems, sensors and actuators [1–3]. For this purpose, SMA thin films have been grown by different techniques like evaporation, sputtering, electrodeposition, etc [1–5]. One of the most important issues is the control of the chemical composition of the alloys, given that small changes in the composition generally induce great shifts in the martensitic transformation temperature ( $M_s$ ). Among all the SMA, films of TiNi-based alloys have been extensively studied [1], but few works have been done towards the potential application of other alloys. In particular Cu-based alloys could be of interest given that they present a narrower hysteresis and a wide range of  $M_s$  temperatures, which can be obtained by small variation in the alloy composition.

Considering the potential application of Cu-based SMA, recently we have shown that in binary Cu–Zn films grown by electrodeposition the martensitic transformation temperature could be tuned during annealing by the control of the Zn vapour pressure by means of a Cu–Zn reference sample [6]. However, in the Cu–Zn alloys,

the maximum achievable transformation temperature is of around 200 K.

Ternary Cu–Zn–Al SMA offers several great advantages compared with binary Cu–Zn. Firstly the inclusion of Al in the alloys allows extending the  $M_s$  temperature range from 0 K to around 700 K. In addition, it is possible to extend the stability field of the  $\beta$  parent phase to lower temperatures with a minimum at a valence electron concentration around 1.48 [7,8]. This permits betatization thermal treatments also at lower temperatures and, moreover, no fast quenching is necessary to keep the  $\beta$  phase in a metastable state at room temperature [9]. Finally it should be mentioned that at least three different martensitic structures can be obtain depending on the alloy composition with a wide range of  $M_s$  for each structure. Each structure offers different mechanical behaviour, particularly different hysteresis width.

In this work, we report a reproducible method to obtain for the first time Cu–Zn–Al thin films with shape memory effect. First binary Cu–Al thin films are obtained by DC sputtering. Afterwards the Zn is added by annealing the Cu–Al films, encapsulated in argon atmosphere, at high temperature and in the presence of a reference Cu–Zn–Al bulk specimen. In this way the Zn vapour pressure is controlled during annealing, and films with a chemical composition very close to the bulk reference composition can be obtained. The structures and microstructures of the as grown films were analysed by X-ray diffraction patterns and transmission electron microscopy. The martensitic transformation temperature was determined by resistivity vs. temperature measurements.

### 2. Experimental

Thin films with a composition of Cu–Al (19.5 at.%) were grown by DC sputtering on Si (100) at room temperature in an atmosphere of

\* Corresponding author at: Comisión Nacional de Energía Atómica, Centro Atómico Bariloche, Bustillo 9500, S. C. de Bariloche, 8400 R. N., Argentina. Tel.: +54 2944445147; fax: +54 2944445299.

E-mail address: [nhaberk@cab.cnea.gov.ar](mailto:nhaberk@cab.cnea.gov.ar) (N. Haberkorn).

10 mTorr of argon. The target was prepared with pure metal melted in an encapsulated quartz tube under argon atmosphere. Deposition sputtering rate was estimated from cross section scanning electron microscope (SEM) images, given a rate of approximately 34 nm/min. After growth the Cu–Al films were easily peeled off from the substrates and encapsulated in quartz tubes in argon atmosphere together with a Cu–Zn–Al bulk reference. These bulk references were prepared in such a way that in both cases the alloys have similar Cu/Al atomic ratio as the sputtering target ( $\approx 4$ ). Reference 1 (BR1) has a concentration Cu – 16 at.%, Zn – 16.7 at.%, Al and reference 2 (BR2) has a concentration Cu – 13.15 at.%, Zn – 17.4 at.%, Al. The films were annealed from room temperature to 1050 K at 5 K/min, and quenched in iced water. Longer annealing at 1050 K (for more of 24 h) or higher temperatures (1173 K) does not show appreciable effects in the martensitic transformation temperature, nor in the hysteresis of the transformation.

Plan view specimens were prepared by Ar ion milling to perforation of films with thicknesses of 1 and 2  $\mu\text{m}$ , at low angle ( $7^\circ$ ) and low energy 2.0 keV in order to avoid structural damage. The films were observed in a Philips CM200UT transmission electron microscope operating at 200 kV, with a spherical aberration coefficient of 0.5 mm and a point resolution of 0.19 nm. The films were characterized by X-ray diffraction and the composition was analysed by energy dispersive spectroscopy (EDS) in scanning electron microscopy (SEM). Electrical transport was measured with the conventional four-probe geometry.

The presence of shape memory in the films was also tested by means of a mechanical deformation in the martensitic structure [5]. An initially flat film, with one end fixed to a Cu plate with Ag paint, was cooled to the martensitic phase and mechanically deformed. Afterwards, it was heated and the evolution of the shape was photographed. The temperature of the film was estimated from thermocouple reading attached to the Cu plate. When the film was heated to a temperature corresponding to the austenitic structure the initial flat shape was recovered.

### 3. Results and discussion

The XRD pattern of a Cu–Al (19.5 at.%) thin films grown by sputtering is shown in Fig. 1. The peaks are indexed as FCC since a XRD pattern in powder obtained by grinding the films shows all the peaks corresponding to this crystalline phase, which is the expected one for the binary alloy at this composition [10]. The films grow textured in the (1 1 1) axis and the rocking curve width of the films is

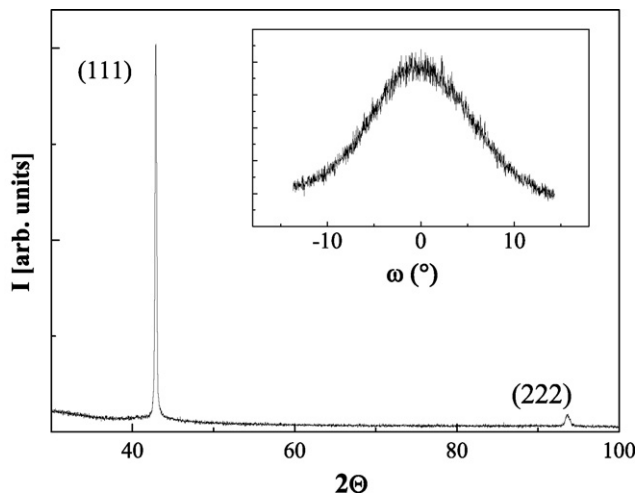


Fig. 1. X-ray diffraction pattern of a Cu–Al film obtained by sputtering. The inset shows the rocking curve of Cu–Al (1 1 1).

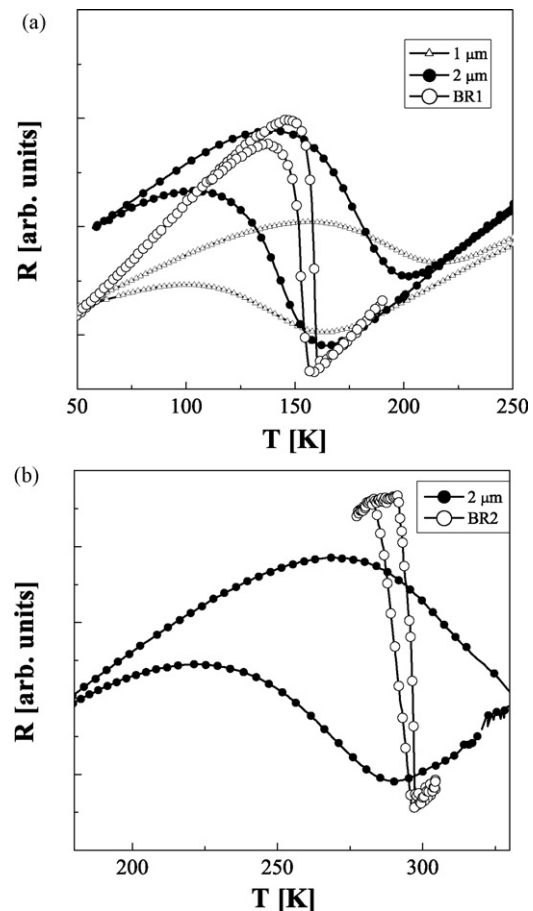


Fig. 2. Resistance vs. temperature in bulk references and annealed films of Cu–Zn–Al during cooling and heating cycles. (a) Films annealed with bulk reference 1 (BR1). (b) Films annealed with bulk reference 2 (BR2). The resistance was rescaled for a clearer presentation.

approximately  $15^\circ$  as shown in the inset of Fig. 1. TEM images show that the sputtered films contain grains with diameter of around 60 nm.

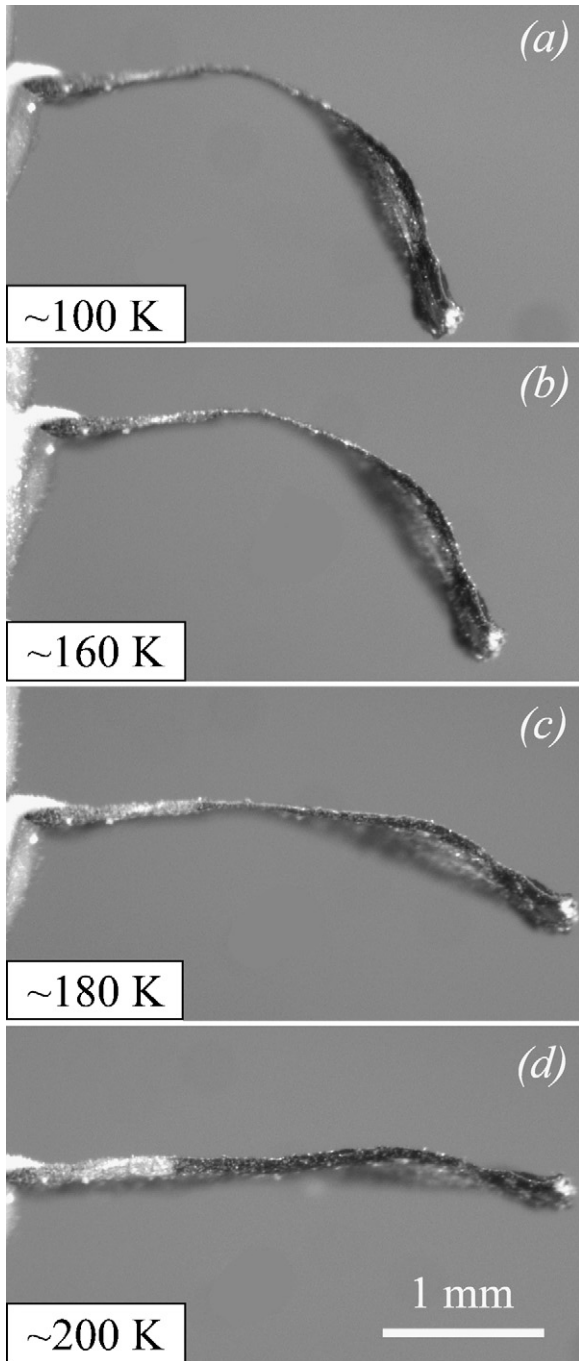
After annealing the films show a Zn chemical composition similar to the bulk reference. Fig. 2 shows resistance vs. temperature measurements for annealed films and bulk references. Fig. 2(a) shows the results for films with thicknesses of 1 and 2  $\mu\text{m}$ , and the BR1 used in the annealing, whereas Fig. 2(b) shows the results for a film with thickness of 2  $\mu\text{m}$ , and the BR2 used in the annealing. After the first thermal cycle the martensitic transformation temperature and the width of the transition did not change during successive thermal cycles. Table 1 shows a summary of the values of the start and finish temperatures for martensite and austenite ( $M_s$ ,  $M_f$ ,  $A_s$  and  $A_f$ ). Since the temperature dependence of the resistance has a very smooth behaviour with no appreciable discontinuity in the slope, these values were estimated following the procedure given in Ref. [11]. The hysteresis was measured as the half-width of the transformation.

The presence of the shape memory effect in the films was also tested by means of a mechanical deformation of an initially flat film in the martensitic phase. Fig. 3 shows the thermal evolution of a 2  $\mu\text{m}$  film annealed with BR1, with  $M_s$  and  $A_s$  of approximately 160 K, as was reported in Table 1. The film was deformed in liquid nitrogen and then heated up. The original flat shape was recovered at approximately 200 K in good agreement with the resistivity measurements (Fig. 2(a) and Table 1). In the case of films annealed with BR2 the original shape was recovered when the films were heated up to room temperature (not showed).

**Table 1**

Transformation temperatures, hysteresis and ranges of transformation of the bulk references BR1 and BR2 and the thin films annealed with each one of them. The values were obtained from the resistivity vs. temperature measurements. The average grain diameter of the observed samples was also included.

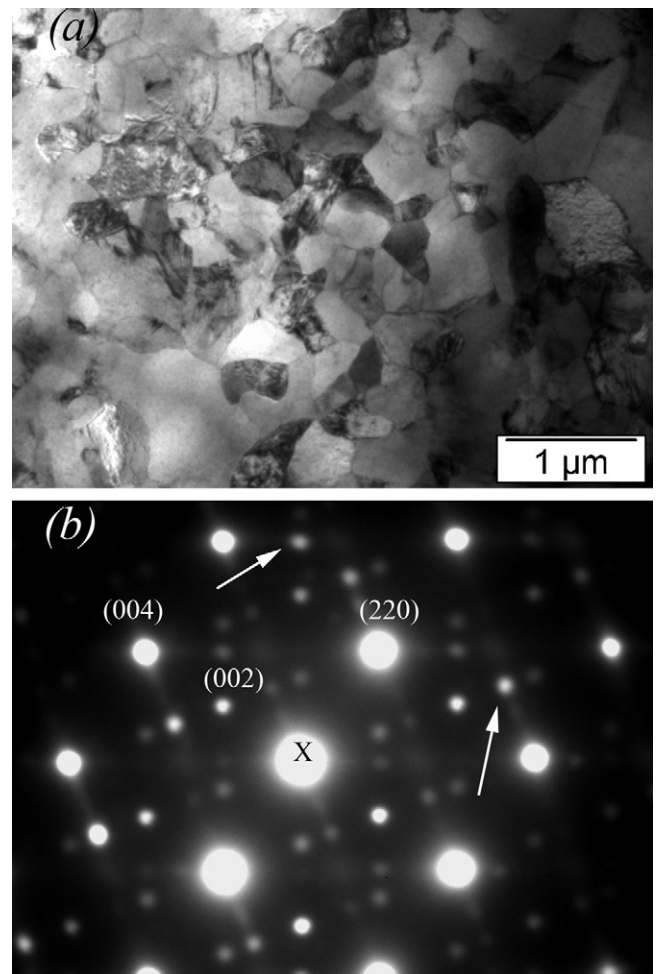
	$A_s$ (K)	$A_f$ (K)	$M_s$ (K)	$M_f$ (K)	$A_f - A_s$ (K)	$M_s - M_f$ (K)	Hysteresis (K)	Average grain diameter ( $\mu\text{m}$ )
BR1	$155 \pm 3$	$160 \pm 2$	$155 \pm 2$	$150 \pm 3$	$5 \pm 4$	$5 \pm 4$	$5 \pm 1$	$1000 \pm 300$
1 $\mu\text{m}$ (BR1)	$155 \pm 5$	$225 \pm 10$	$165 \pm 5$	$95 \pm 10$	$65 \pm 12$	$70 \pm 12$	$55 \pm 2$	$0.5 \pm 0.2$
2 $\mu\text{m}$ (BR1)	$160 \pm 3$	$200 \pm 5$	$160 \pm 3$	$110 \pm 10$	$40 \pm 6$	$45 \pm 11$	$35 \pm 2$	–
BR2	$295 \pm 2$	$300 \pm 2$	$295 \pm 2$	$285 \pm 3$	$5 \pm 4$	$10 \pm 4$	$5 \pm 1$	$1000 \pm 300$
2 $\mu\text{m}$ (BR2)	$275 \pm 5$	$330 \pm 5$	$290 \pm 5$	$220 \pm 10$	$50 \pm 7$	$70 \pm 11$	$40 \pm 2$	$1.0 \pm 0.4$



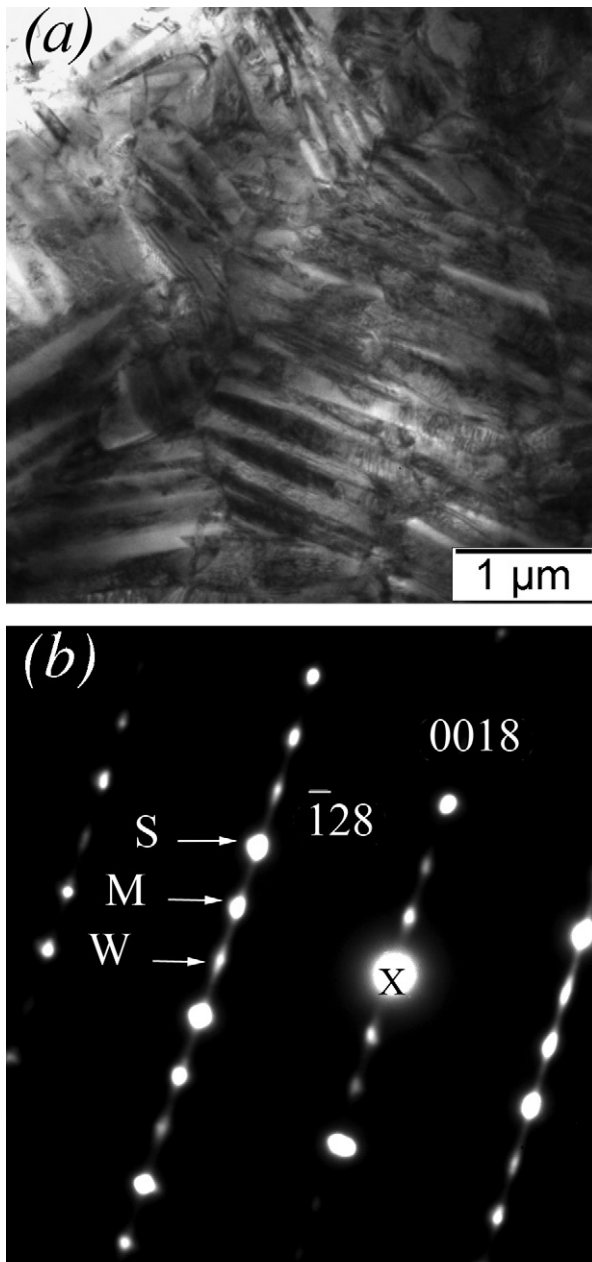
**Fig. 3.** Thermal evolution of an initially flat film deformed in liquid nitrogen. (a) At  $\sim 100$  K no recovery is observed. (b) Start of shape recovery at  $\sim 160$  K. (c) Partially recovered shape at  $\sim 180$  K. (d) Recovered flat film at  $\sim 200$  K.

Fig. 4(a) shows a TEM image of the microstructure of a film of 1  $\mu\text{m}$  annealed with BR1. The film has an average grain diameter of 500 nm with grains as large as 1  $\mu\text{m}$ . Fig. 4(b) shows a diffraction pattern corresponding to one grain in Fig. 4(a) oriented along the  $[1\bar{1}0]$  zone axis of the  $\beta$  phase with  $L2_1$  structure. We do not observe the presence of  $\alpha$  or  $\gamma$  precipitates in the sample. Additional spots indicated by arrows correspond to a thin layer ( $<7$  nm) of surface martensite that forms spontaneously in the copper based alloys, being dependent on the surface orientation [12].

Fig. 5(a) shows a TEM image of a film of 2  $\mu\text{m}$  annealed with the BR2. This film is in martensitic phase at room temperature when it is heated from low temperatures. The image shows small martensitic plates with a width of around 200 nm in the grains with an average diameter of 1  $\mu\text{m}$ . The electron diffraction pattern corresponding to the 18R structure is shown in Fig. 5(b).



**Fig. 4.** (a) Bright field image of the microstructure of a film of 1  $\mu\text{m}$  annealed with BR1. (b) Diffraction pattern of  $\beta$  phase ( $L2_1$  structure) in the zone axis  $[1\bar{1}0]$  corresponding to one grain in (a). Spots of the type indicated by arrows correspond to reflection from surface martensite [11].



**Fig. 5.** (a) Bright field image of the microstructure of a film of 2 μm annealed with BR2. (b) Corresponding electron diffraction pattern of the 18R martensite along the  $[2\ 1\ 0]_{18R}$  orientation. The typical sequence strong (S), medium (M) and weak (W) intensity of the spots along the *c* axis is indicated.

The crystalline structure of the martensite in Cu–Zn–Al alloys depends on the electron concentration  $e/a$ , which is the average number of conduction electrons per atom. In this work,  $e/a$  are 1.49 and 1.48 for BR1 and BR2 respectively. Thus the presence of the 18R structure is indeed expected for these  $e/a$  [13]. Although small temperature hysteresis is expected between  $\beta$  and the 18R structure, as actually observed in the bulk reference specimens BR1 and BR2, a large hysteresis is observed in the thin films (see Fig. 2 and Table 1). In addition the thin film samples show  $M_s$  and  $A_s$  values very close to the bulk references, however  $M_f$  and  $A_f$  were significantly lower and higher respectively for the thin films. This is due to

the extended range of transformation ( $A_f - A_s$  and  $M_s - M_f$ ) present in the thin films. These phenomena, the wider hysteresis and the more extended transformation range, are more likely related to the grain diameter. Similar behaviour was observed in bulk polycrystalline CuAlBe, in stress induced transformation, where the transformation stress and the pseudoelastic slope were studied as a function of the grain diameter [14]. The wider hysteresis and the more extended transformation could be attributed to the energy delivered and stored in the material, by plastic and elastic deformation respectively, due to the grain boundaries accommodation upon the shape change associated to the martensitic transformation. In addition some inhomogeneities in chemical composition of the Cu–Al films obtained by sputtering may also take place in the thin films [6], increasing the temperature transformation range.

#### 4. Conclusion

Cu–Zn–Al films showing martensitic transformation have been grown in two steps: first, films of Cu–Al have been grown by sputtering and second, the Cu–Al films have been annealed in a sealed quartz capsule with argon atmosphere, in presence of a Cu–Zn–Al bulk reference to fix the Zn vapour pressure. From the same initial Cu–Al films different  $M_s$  transformation temperatures could be obtained by adding Zn to the films according to the Zn vapour pressure during the annealing. The films in  $\beta$  phase have  $L2_1$  structure and in the martensitic state present the 18R structure, as expected from the chemical composition. The films show an  $M_s$  transformation temperature very close to the bulk references  $M_s$ . This means they have similar chemical composition. A relationship between the grain diameters, the hysteresis and the transformation range was found. The smaller the grain diameter the larger the hysteresis width and the temperature transformation range.

#### Acknowledgments

We thank to Enrique Aburto and Matías Isla for technical assistance in the encapsulation of samples in quartz tubes. This work has been supported by Agencia Nacional de Promoción Científica y Tecnológica. PICT 2007-00327, PICT 2004-20144, and CONICET PIP 5657. N.H., A.M.C. and J.G. are member of CONICET.

#### References

- [1] Y.Q. Fu, H.J. Du, W.M. Huang, S. Zhang, M. Hu, *Sens. Actuators A: Phys.* 112 (2004) 395–408.
- [2] M. Cai, S.C. Langford, M. Wu, W. Huang, G. Xiong, T.C. Droubay, A.G. Joly, K.M. Beck, W.P. Hess, J.T. Dickinson, *Adv. Funct. Mater.* 17 (2007) 161–167.
- [3] H. Kahny, M.A. Huffz, A.H. Heuery, *J. Micromech. Microeng.* 8 (1998) 213–221.
- [4] F. Wang, S. Doi, K. Hosoi, H. Yoshida, T. Kuzushima, M. Sasaki, T. Watanabe, *Electrochim. Acta* 51 (2006) 4250–4254.
- [5] F.C. Lovey, A.M. Condó, J. Guimpel, M.J. Yacamán, *Mater. Sci. Eng. A* 481–482 (2008) 426.
- [6] N. Haberkorn, M. Ahlers, F. Lovey, *Scripta Mater.* 61 (2009) 821–824.
- [7] M. Ahlers, *Prog. Mater. Sci.* 30 (1986) 135–186.
- [8] M. Ahlers, *Scripta Metall.* 8 (1974) 213–316.
- [9] F.C. Lovey, V. Torra, *Prog. Mater. Sci.* 44 (3) (1999) 189–289.
- [10] J.L. Murray, *Int. Metals Rev.* 30 (1985) 211.
- [11] P. Krulevitch, A.P. Lee, P.B. Ramsey, J.C. Trevino, J. Hamilton, NorthpF A.M., *J. Microelectromech. Syst.* 5 (4) (1996) 270–282.
- [12] (a) F. Lovey, M. Chandrasekaran, R. Rapacioli, M. Ahlers, *Z. Metallkde* 71 (1980) 37–41;  
(b) F. Lovey, M. Chandrasekaran, *Acta Metall.* 31 (1983) 1919–1927.
- [13] (a) J.L. Peregrina, M. Ahlers, *Acta Metall. Mater.* 40 (1992) 3205–3211;  
(b) F. Saule, M. Ahlers, F. Kropff, E.B. Rivero, *Acta Metall. Mater.* 40 (1992) 3238–3329.
- [14] S. Montecinos, A. Cuniberti, A. Sepúlveda, *Mater. Charact.* 59 (2008) 117–123.